PAPER Special Issue on Mobile Communication Antennas

Analysis on Small Planar Antenna in a Paging System

Nozomu ISHII† *and* Kiyohiko ITOH†, *Members*

SUMMARY In this paper, the characteristics of the card-sized paging antenna composed of plates and wires are estimated in view of its efficiency. To analyze this type of antennas using the reaction matching technique for the wire antenna, we approximate the plate parts to the wire grids. In the analysis of the antenna with a complex configuration, the numerical input impedance by the usual reaction technique assumed the local symmetry in calculating one mutual impedance, is sometimes incorrect. Therefore, we carry out the reaction matching on the condition that the dipoles are placed at their own positions throughout calculating the mutual impedances. In modeling the plate with a wire-grid, we estimate the loss effect of the plate parts by introducing the equivalent radius. Furthermore, we examine the validity of the wire-grid model for the card-sized antenna. And, we estimate the radiation efficiency as a function of the gap distance of the plates, and discuss the polarization matching and the impedance matching of the thin paging antenna, in view of the total efficiency.

1. Introduction

Antennas for the mobile communication are required to be small and thin for the reason of the mobility. It is said that the electrical performance of such antennas grows worse, as they become smaller and thinner[1]. The typical antenna using in the paging system has two card-sized conducting plates as shown in Fig. 1. In this configuration, the gap between the plate and the ground plane must be very narrow for the design restriction so that the antenna efficiency would become very small. Furthermore, owing to the small size of the antenna, the natural resonant frequency of this configuration is largely different from the operating frequency. In spite of such a drawback, this type of antenna was developed by means of an experimental approach based on a social demand; however, the corresponding numerical methods have not been established enough to analyze these performances until now.

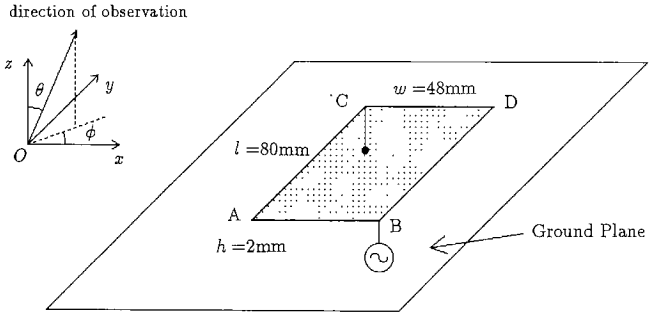

Fig. 1 The thin card-sized planar antenna for the paging.

Newman and Pozar analyzed an antenna of composite wire and plate geometry[2]. In their method, the current flowed on antenna is expressed by a thin-wire mode, a surface patch mode, and an attachment mode, and it is required to estimate the mutual impedances between two modes. For this reason, their method is complex. Therefore, in this paper, we approximate the plane parts with a wire-grid model[3], and we expand this antenna with piecewise sinusoidal thin-wire mode. And we apply the method of moments which is based on the reaction integral equation for this model. The mutual impedance between two piecewise sinusoidal thin-wire modes is precisely estimated by Amano et al.[4] for two dimensional problems, by Richmond et al.[5] and Tilston et al.[6] for three dimensional problems. In this paper, we use their methods to find the mutual impedance. Sato et al. analyzed the inverted-F antenna on the rectangular conducting body using the wire-grid model[7]. Also, Morishita et al. dealt with the MSA which has small antenna height, approximating the ground plane to a corresponding wire-grid model[8]. However, the analysis for the small planar antenna, which the antenna height h is extremely small (h is nearly equal to $\lambda/300$), has not been reported yet. Therefore, the analysis of the card-sized paging antenna in this paper is very meaningful.

Taking the above discussion into consideration, first, we will explain the numerical method for the wire antennas used in this paper, and discuss about the offset between the expansion dipole and the test dipole. Next, we will examine the validity of modeling the plate with the corresponding wire grids. Moreover, we will compute and consider the characteristics of the planar loop antenna for the card-sized paging, with the view of the total efficiency of the antenna system.

Manuscript received April 15, 1991.
Manuscript revised June 22, 1991.
† The authors are with the Faculty of Engineering, Hokkaido University, Sapporo-shi, 060 Japan.

2. Analysis Method for Wire Antennas

"Method of moments based on the reaction integral equation", proposed by Richmond[9] is well known as an unified approach for the antennas constructed by the wire components, or plate components with wire-grid. We will present this formulation below. Assuming electromagnetic distribution on the surface of the scatterers and test source inside the conductor, the following "Rumsey zero reaction theorem"[10] holds,

$$\oiint_S (\boldsymbol{J}^s \cdot \boldsymbol{E}^t - \boldsymbol{M}^s \cdot \boldsymbol{H}^t)\, dS + \iiint (\boldsymbol{J}^i \cdot \boldsymbol{E}^t - \boldsymbol{M}^i \cdot \boldsymbol{H}^t)\, dV = 0, \quad (1)$$

where $(\boldsymbol{J}^s, \boldsymbol{M}^s)$ are the electric and magnetic surface-current densities on the closed surface S of scatterer, $(\boldsymbol{J}^i, \boldsymbol{M}^i)$ are the electric and magnetic source-current densities, and $(\boldsymbol{E}^t, \boldsymbol{H}^t)$ are the free-space electric and magnetic fields of test sources.

Equation (1) is the integral equation for the scattering problem, and our goal is to determine the surface-current $(\boldsymbol{J}^s, \boldsymbol{M}^s)$ using this equation. To achieve our purpose, we expand these current densities in finite series. Hence, there will be a finite number N of unknown expansion coefficients. Next, we should obtain N simultaneous linear equations to obtain these coefficients. Each equation is obtained from Eq. (1) each time we set up new test source.

We assume that the conductor has a finite conductivity and satisfies the impedance boundary condition as follows:

$$\boldsymbol{M}^s = Z_s \boldsymbol{J}^s \times \hat{n}, \quad (2)$$

where Z_s denotes the surface impedance. The unit vector $\hat{n}$ is directed outward on S. If $\boldsymbol{M}^i$ vanishes, Eqs. (1) and (2) yield,

$$-\iint_S \boldsymbol{J}^s \cdot [\boldsymbol{E}_m - (\hat{n} \times \boldsymbol{H}_m) Z_s]\, dS = \iiint \boldsymbol{J}^i \cdot \boldsymbol{E}_m\, dS, \quad (3)$$

where $(\boldsymbol{E}_m, \boldsymbol{H}_m)$ denote the free-space electric and magnetic fields of test-sources m.

We divide the scatterer into suitable dipoles, and express it as the superposition of V-shaped dipoles. Namely, we expand the electric current distribution $\boldsymbol{J}^s$ in known expansion functions $\boldsymbol{J}_n$:

$$\boldsymbol{J}^s = \sum_{n=1}^{N} I_n \boldsymbol{J}_n, \quad (4)$$

where the complex coefficient I_n is a sample value of function $\boldsymbol{J}_n$. And we use the expansion function $\boldsymbol{J}_n$ with unit current density at the terminals. From Eqs. (3) and (4), we obtain the simultaneous linear equations:

$$\sum_{n=1}^{N} Z_{mm} I_n = Vm \quad \text{for} \quad m = 1, 2, 3, \cdots, N, \quad (5)$$

where

$$Z_{mm} = -\iint_n \boldsymbol{J}_n \cdot [\boldsymbol{E}_m - (\hat{n} \times \boldsymbol{H}_m) Z_s]\, dS, \quad (6)$$

$$V_m = \iiint_i \boldsymbol{J}^i \cdot \boldsymbol{E}_m\, dV = \iint_m \boldsymbol{J}_m \cdot \boldsymbol{E}^i\, dS. \quad (7)$$

In Eq. (7), the second equality is guaranteed by the reciprocity theorem and $\boldsymbol{E}^i$ denotes the impressed electric field. The region n extends over a part of the surface S where the expansion function $\boldsymbol{J}_n$ is non-zero, and the region m includes the interior test function $\boldsymbol{J}_m$. In this paper, according to the Galerkin's method, we choose the same functions as the expansion functions $\boldsymbol{J}_n$ for the test functions $\boldsymbol{J}_m$. Therefore, it is required to evaluate the mutual impedance Z_{mn} between these V-shaped dipoles as shown in Fig. 2.

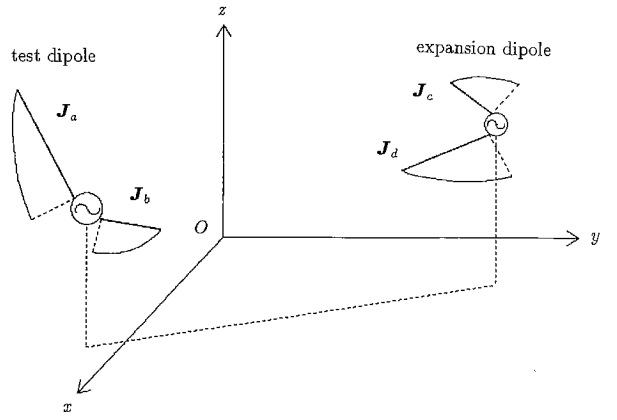

Fig. 2 Two V-shaped dipoles having arbitrary inclinations and bending angle.

In this paper, we assume that the antenna has a finite conductivity. To simplify the discussion, however, we assume that the antenna consists of a perfect conductor for the most part in this section. In the last part of this section, we will explain the treatment of the lossy antenna, briefly.

Now, we will explain the calculation of the mutual impedance between the piecewise sinusoidal dipoles. Since each dipole is composed of two monopoles, the sum of the fields produced by the two monopoles gives the field of the dipole. We will dismantle a certain dipole into the corresponding two monopoles which have the test surface current distribution, $\boldsymbol{J}_a$, $\boldsymbol{J}_b$, respectively. Except a constant, the surface current distribution on the test dipole $\boldsymbol{J}_m$, is given as follows:

$$\boldsymbol{J}_m = \boldsymbol{J}_a + \boldsymbol{J}_b, \quad (8)$$

where $\boldsymbol{J}_a$, $\boldsymbol{J}_b$ are given as follows, introducing the local cylindrical coordinate (ρ, ϕ, z) for each monopole,

$$\boldsymbol{J}_a=\frac{\hat{z}_a}{2\pi r_a}\cdot\frac{\sin k(\Delta z_a-z)}{\sin k\Delta z_a}, \tag{9a}$$

$$\boldsymbol{J}_b=\frac{\hat{z}_b}{2\pi r_b}\cdot\frac{\sin k(\Delta z_b+z)}{\sin k\Delta z_b}, \tag{9b}$$

where $\hat{z}_a$, $\hat{z}_b$ denote the unit vectors directed to each monopole axis, Δz_a, Δz_b denote the length of each monopole, and r_a, r_b denote the radii of each monopole. Therefore, the field of this dipole is given as follows:

$$\boldsymbol{E}_m=\boldsymbol{E}_a+\boldsymbol{E}_b, \tag{10a}$$

where

$$\boldsymbol{E}_i=-j\omega\mu\left[\bar{\boldsymbol{I}}+\frac{1}{k^2}\nabla\nabla\right]\cdot\iint\frac{e^{-jk|\boldsymbol{r}-\boldsymbol{r}'|}}{4\pi|\boldsymbol{r}-\boldsymbol{r}'|}\boldsymbol{J}_i(\boldsymbol{r}')\,dS' \quad \text{for } i=a, b, \tag{10b}$$

where $\bar{\boldsymbol{I}}$ is a unit dyad which can be represented by a unit diagonal matrix.

On the other hand, the expansion dipole can be also taken apart into two monopoles. The expansion surface current density $\boldsymbol{J}_n$ can be given as follows:

$$\boldsymbol{J}_n=\boldsymbol{J}_c+\boldsymbol{J}_d. \tag{11}$$

Therefore, the mutual impedance can be found using Eqs. (6), (10a), and (11):

$$\begin{aligned}Z_{mn}&=-\iint_n\boldsymbol{J}_n\cdot\boldsymbol{E}_m dS\\&=-\iint_c\boldsymbol{J}_c\cdot\boldsymbol{E}_a dS-\iint_c\boldsymbol{J}_c\cdot\boldsymbol{E}_b dS\\&\quad-\iint_d\boldsymbol{J}_d\cdot\boldsymbol{E}_a dS-\iint_d\boldsymbol{J}_d\cdot\boldsymbol{E}_b dS.\end{aligned} \tag{12}$$

Thus, it is required to calculate four mutual impedances between the two monopoles and then superpose them, in order to evaluate the mutual impedance between the two dipoles.

Consider the monopole-monopole mutual impedance between # a and # c (See Fig. 3):

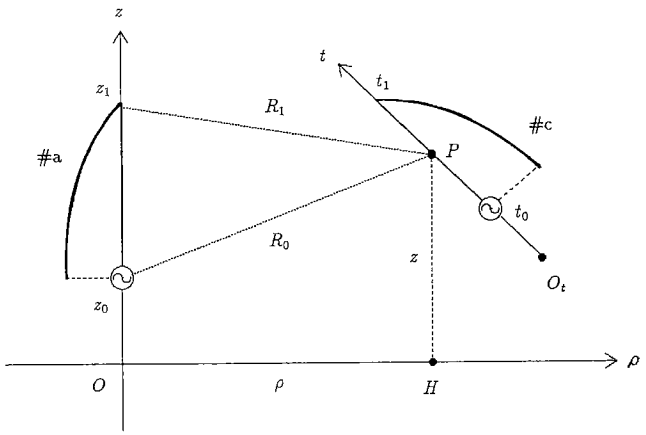

Fig. 3 The local cylindrical coordinate for the calculation of the mutual impedance between the monopoles.

$$Z_{ac}=-\iint_c\boldsymbol{J}_c\cdot\boldsymbol{E}_a dS. \tag{13}$$

In the local cylindrical coordinate for the monopole # a, $\boldsymbol{E}_a$ can be given as follows:

$$\boldsymbol{E}_a=\hat{\rho}E_{a\rho}(\rho, z)+\hat{z}\,E_{az}(\rho, z), \tag{14}$$

where

$$\begin{aligned}E_{a\rho}(\rho, z)=\frac{j\eta}{4\pi\rho}\Bigg[&\frac{z-z_1}{\sin k\Delta z}\cdot\frac{e^{-jkR_1}}{R_1}\\&-\frac{(z-z_0)\cos k\Delta z}{\sin k\Delta z}\cdot\frac{e^{-jkR_0}}{R_0}-je^{-jkR_0}\\&+j\rho^2\frac{e^{-jkR_0}}{R_0^2}+\frac{\rho^2}{k}\frac{e^{-jkR_0}}{R_0^3}\Bigg],\end{aligned} \tag{15a}$$

$$\begin{aligned}E_{az}(\rho, z)=\frac{j\eta}{4\pi}\Bigg[&-\frac{1}{\sin k\Delta z}\cdot\frac{e^{-jkR_1}}{R_1}\\&+\frac{\cos k\Delta z}{\sin k\Delta z}\cdot\frac{e^{-jkR_0}}{R_0}\\&+j(z-z_0)\frac{e^{-jkR_0}}{R_0^2}+\frac{z-z_0}{k}\frac{e^{-jkR_0}}{R_0^3}\Bigg],\end{aligned} \tag{15b}$$

and $R_i=\sqrt{\rho^2+(z-z_i)^2}$, $i=0, 1$, $\eta=\sqrt{\mu/\varepsilon}$, $\Delta z=z_1-z_0$, and $\hat{\rho}$, $\hat{z}$ denote the radial and z-directed unit vectors in this local coordinate[5]. The integral of Eq. (13), which must be evaluated strictly on the surface of # c, can be given on the assumption that the cross-sectional current distribution is uniform:

$$\begin{aligned}Z_{ac}=-\int_{t_0}^{t_1}I_c(t)\{&(\hat{t}\cdot\hat{\rho})E_{a\rho}(\rho, z)\\&+(\hat{t}\cdot\hat{z})E_{az}(\rho, z)\}dt,\end{aligned} \tag{16}$$

where

$$I_c(t)=\frac{\sin k(t_1-t)}{\sin k(t_1-t_0)}, \tag{17}$$

and $\hat{t}$ is the unit vector directed to the axis of the monopoles # c. Note that $I_c(t)$ is related to the expansion monopole $\boldsymbol{J}_c$, and I_n in Eq. (4) is the current coefficient of the dipole $\boldsymbol{J}_n$ which is the sum of the monopoles $\boldsymbol{J}_c$ and $\boldsymbol{J}_d$. To integrate Eq. (16) numerically and obtain the mutual impedance Z_{ac}, it is required that ρ, z, and $\hat{\rho}$ in the integrand of Eq. (16) is explicitly expressed in terms of t. These three variables are given as follows:

$$z=\overrightarrow{OP}\cdot\hat{z}, \tag{18a}$$

$$\rho=|\overrightarrow{OH}|, \tag{18b}$$

$$\hat{\rho}=\overrightarrow{OH}/\rho, \tag{18c}$$

where $\overrightarrow{OP}=\overrightarrow{OO_t}+t\,\hat{t}$ and $\overrightarrow{OH}=\overrightarrow{OP}-z\,\hat{z}$ as shown in Fig. 3.

The expansion functions are set up as overlapping tubular piecewise sinusoidal surface currents, and the

filamentary currents which are parallel to the tubular surface currents, are used as the test functions. Since the cross-sectional distribution of the expansion currents is different from that of the test currents, the mutual impedance is not always satisfied with the symmetry or the reciprocity. Therefore, there is a possibility that the reaction between the tubular expansion monopole # c and the filamentary test monopole # a is not equal to that between the tubular expansion monopole # a and the filamentary test monopole # c[6]. This asymmetry occurs between two monopoles which have the different arm lengths and no coincident axis.

In this paper, throughout the calculation of the mutual impedances, the locations of the expansion dipoles and the test dipoles are fixed. Therefore, the reciprocity theorem is often not satisfied. However, the numerical antenna impedance agrees with the experimental impedance, because the reaction theorem holds physically over the whole antenna. On the other hand, according to the usual method proposed by Richmond et al.[5],[6],[9], the expansion dipole and the test dipole are set to be satisfied with the local reciprocity for one mutual impedance calculation. But, using the usual method, numerical impedance is often largely different from the experimental one. There are two reasons for this disagreement. First, the expansion functions do not present the practical current exactly. Second, the point charges are generated at the wire junctions for the discontinuities of the expansion functions. These discontinuities result from the dipoles tilting each time the mutual impedance is calculated.

In this paper, we will treat the complex antenna with many branches such as a wire-grid model. In this case, we can satisfy the Kirchhoff's current law by setting the V-shaped dipoles as shown in Fig. 4. In general, at the node with n branches, $(n-1)$ independent V-dipoles are required.

If the antenna has a finite conductivity, the mutual impedance is evaluated according to Eq. (3). In the case of the good conductor $(\sigma \gg \omega\epsilon)$, the surface impedance in Eg. (3) is given as follows:

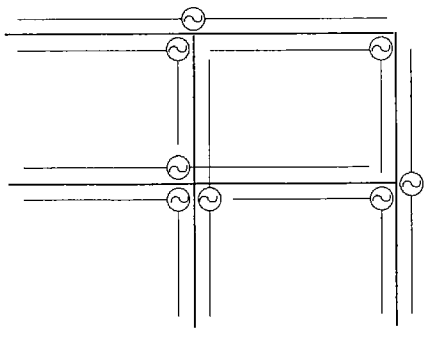

Fig. 4 An example of the dipole placement for the branch configuration.

$$Z_s = (1+j)\sqrt{\frac{\omega\mu}{\sigma}} \tag{19}$$

where σ is the conductivity of the antenna material. If the plate is approximated by the wire-grid model, it is necessary to take into account the loss effect of the plate (the strip with the width w is equivalent to a wire with radius $w/4$[11]).

3. Analysis of Card-Sized Planar Antenna

In this section, we examine the performance of a simple model as shown in Fig. 1, in view of the efficiency. In this figure, the antenna is placed on the ground plane so that it is necessary to consider the image part of this antenna. The efficiency of the antenna system is given as the product of the radiation efficiency, the polarization match factor, and the impedance match factor. Hence, we will discuss the relation between the radiation efficiency and the antenna height h, the method that makes the polarization of the incoming wave to coincide with the maximum pattern direction, and the total characteristics of the system with a simple matching network.

Before dealing with these items, we examine the validity of the wire-grid modeling. Wire grid modeling is justified when it is clear to find a proper choice of the wire diameters and grid size. Despite the fact that no electric field exists inside or on the conductor, the evanescent reactive field clings to both side of the grid which approximates the surface of the conductor. Thus, it is necessary to perturb the interval of the grid and the radius of the wire and for its average to equal the practical current and charge excited on the real continuous surface. In fact, for the small planar antenna, the input impedance depends on the grid size and wire radius choice.

For example, we consider the wire-grid model for the card-sized paging antenna as shown in Fig. 1. This antenna is composed of a rectangular sheet copper having $l=80$ mm length and $w=48$ mm width and two wires with $h=2.0$ mm height. These sheet and wires are connected at two corners of sheet, one (Point C) is shorted and the other (Point B) is fed. A sample of the wire-grid model for this antenna is shown in Fig. 5. This model is an approximation model divided into three parts for the x direction and five parts for the y direction.

To examine the effect of the wire radius, we calculate the relation between the radius and the input impedance. Here, the expansion dipoles are placed above (or beneath) the grid plane shifting with their radius. This numerical result is shown in Fig. 6. As seen in Fig. 6, the values of the resistance and reactance are larger, as the radius grows thicker. In particular, the reactance is increased to 5-20 Ω by 0.2 mm increment of the radius. Thus, the effect of the wire radius

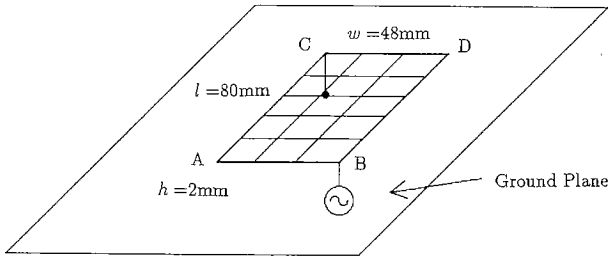

Fig. 5 The wire grid model for thin planar antenna shown in Fig. 1.

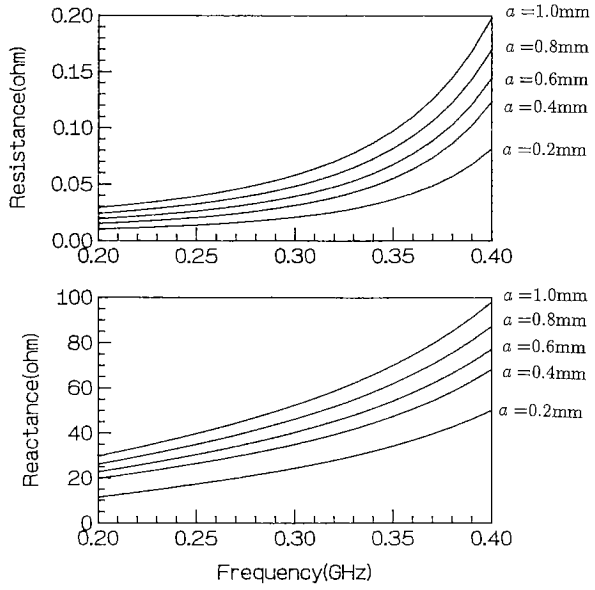

Fig. 6 The relation between the radius of wire-grid and the input impedance for the model as shown in Fig. 5.

becomes a serious problem in modeling the antenna geometry with a wire-grid. Also, the grid size effects on the resonant frequency. In general, the division numbers for the x and y directions should be larger in order to obtain the good results.

Next, we consider the input impedance frequency performance of the antenna shown in Fig. 1 to examine the validity of the method described in Sect. 2. The measured input impedance for this antenna is shown in Fig. 7. The input impedance for the corresponding wire-grid model with 0.6 mm radius (Fig. 5) are given in Fig. 8. From Figs. 7 and 8, the resonant frequencies are 538 MHz for the original model, and 530 MHz for the wire grid model, thus it may be seen that there is only about 8 MHz difference of two models. Besides, it is found that the shapes of these impedance loci are similar to each other. From these reasons, we can approximate the characteristics of the planar antenna shown in Fig. 1 to that of the wire grid model shown in Fig. 5. In the rest of this section, we use the wire-grid model shown in Fig. 5 to compute the characteristic of the original model shown in Fig. 1.

First, we examine the relation of the height h and

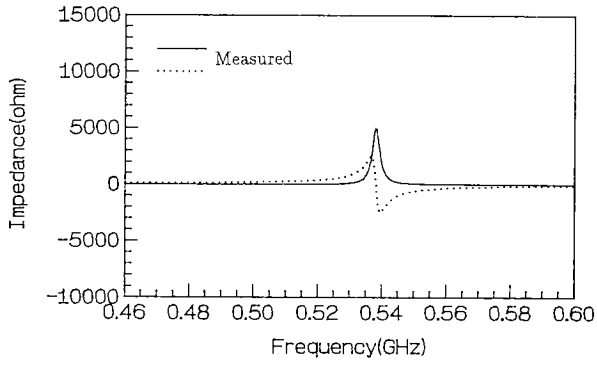

Fig. 7 Input impedance vs. frequency for the antenna shown in Fig. 1. In this figure, the solid and dotted lines denote the real and imaginary parts of the measured impedance respectively.

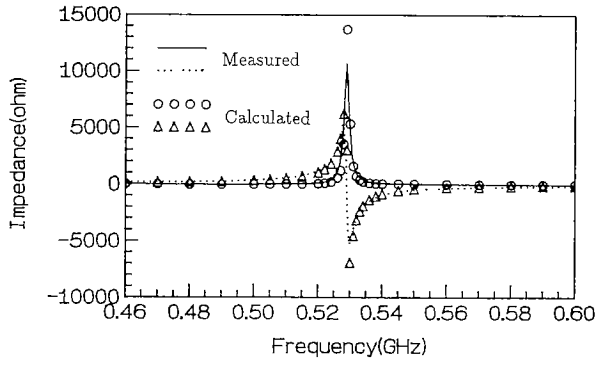

Fig. 8 Input impedance vs. frequency for the wire gird model shown in Fig. 5. In this figure, the solid and dotted lines denote the real and imaginary parts of the measured impedance respectively, and the marks ○, △ denote the real and imaginary parts of the calculated impedance respectively.

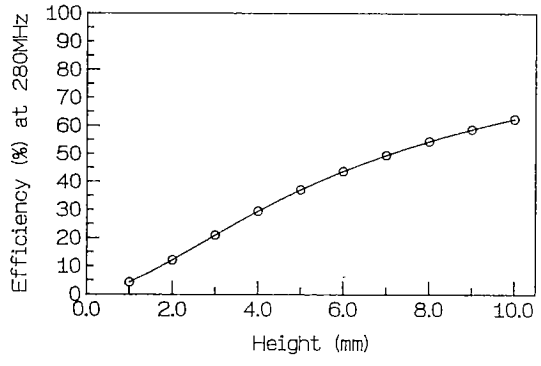

Fig. 9 The antenna height h vs. the radiation efficiency.

the radiation efficiency at 280 MHz for the antenna which is fed at B, and shorted at C shown in Fig. 1. The result is shown in Fig. 9. From this figure, it may be seen that the radiation efficiency or the receiving sensitivity are more remarkably improved as h grows larger.

Second, consider the control of the polarization

plane. Since the antenna shown in Fig. 1 is generally used with the x-y plane directed vertically, it is necessary to design the antenna pattern as the incoming wave vertically polarized is received with the best efficiency. From Fig. 10, in the case of B fed and C shorted, it is observed that the receiving efficiency is maximal when the incoming wave is polarized in the BC direction. Now, consider two cases with x axis directed horizontally and vertically. As seen from Fig. 10, the incoming wave is better received in the former case than in the latter case. Because the receiver is required to maintain the good receiving condition at all times, we should design the pattern to receive in the latter case.

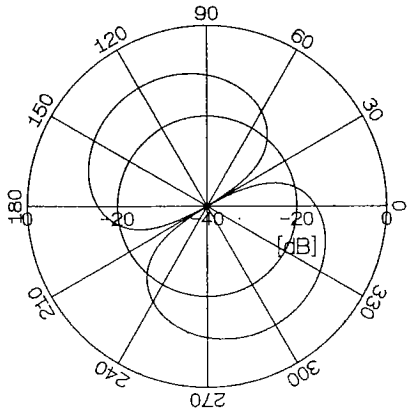

Fig. 10 The pattern observed from $+z$ direction (B fed, C shorted).

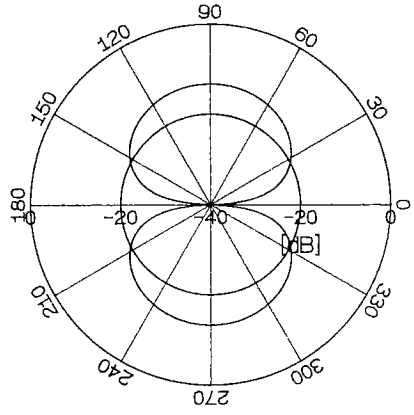

Fig. 11 The pattern observed from $+z$ direction (A, B fed with in-phase excitation, C, D shorted).

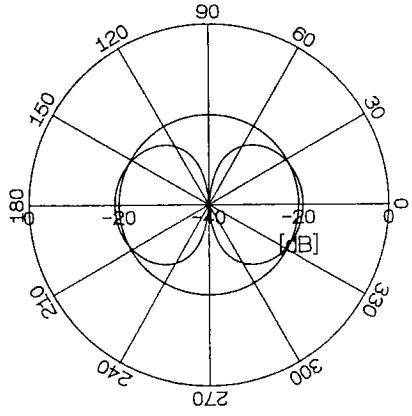

Fig. 12 The pattern observed from $+z$ direction (A, B fed with anti-phase excitation, C, D shorted).

This problem is resolved by the electrical control of the polarization plane with A, B fed and C, D shorted in Fig. 1. If A and B are fed with the same amplitude and phase, the y directed wave is received under the best condition as shown in Fig. 11. Also, if A and B are fed with the same amplitude but with the opposite phase, the x directed wave is received very well as shown in Fig. 12. Thus, by shifting the receiving voltage at A or B to 0° or 180°, the receiver can operate well whenever it is placed vertically or horizontally to the ground.

Finally, we consider the impedance matching at the feeding point of the antenna. Since the impedance of the small antenna is generally low resistive and high reactive, the efficiency is small so that it is necessary to match them at the feeding point. As the matching network, we use the L-section network composed of two capacitors[12] (See Fig. 13).

In the Fig. 14, the efficiencies of the case B fed and

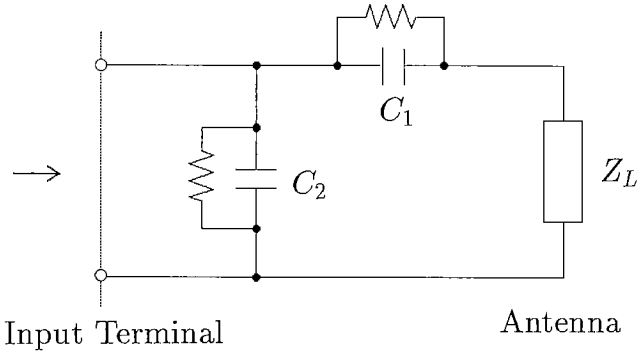

Fig. 13 The L section network using two capacitors with the dielectric loss.

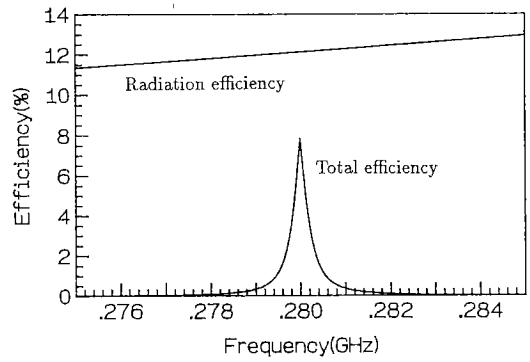

Fig. 14 Efficiency vs. frequency.
The element values of the capacitors used in the L section network are given as follows: $C_1=16.48$[pF], $C_2=355.61$[pF], where $\tan\delta=0.0005$.

C shorted are shown. The line near 12% denotes a radiation efficiency and another line denotes the total efficiency of the antenna system including the matching network, assuming the dielectric loss tangent of the capacitors is equal to 0.0005. At operating frequency (280 MHz), the total efficiency is equal to about 64% of the radiation efficiency. The effect of inserting the matching network in the system is extremely remarkable, for the total efficiency without the matching network is nearly equal to zero because of the very small resistance. In the modern paging system in Japan, 25 kHz is assigned for a channel, therefore 6 MHz for 240 channels are assigned for this system. In general, it is impossible to match such a system within this band using the L section network composed of two fixed capacitors. To overcome this drawback, it is required that this band (6 MHz) be divided into three or six bands (2 MHz or 1 MHz) and the matching is accomplished within each band. As seen in Fig. 14, the band width of over 1% for the total efficiency is nearly equal to 1 MHz. Therefore, to maintain more than 1% efficiency through the band width for the paging system, we must use six L sectional matching networks. If it is possible to use the variable capacitors in the L section network, we can tune them in to each channel in this system.

4. Conclusion

Our objective in this paper is the theoretical estimation of the performances for the card-sized paging antenna. To accomplish this, first, we investigate the moment method which the integral equation for the wire antenna problem is converted to the matrix equation for the numerical computation, and we obtain the current distribution on the antenna by solving this matrix equation. We obtain the available results for the complex antenna such as a wire grid model by placing the dipoles on fixed locations. Also, we estimate the characteristics of the planar loop antenna used in the paging system by means of the wire grid modeling. We show that if one corner of the plate is shorted and the other one is fed, the pattern is directed to the line that links their two corners. It is confirmed that when the height of the antenna height is higher, the efficiency is much better. And we discuss the electric pattern control by two point feed. Moreover in view of the total efficiency, we examine the impedance matching and it has been found that the L section network composed of two capacitor is applicable to the antennas becoming widespread in the modern paging system.

Acknowledgements

This work was supported by Grant-in-Aid for Scientific Research 62420033 from the ministry of Education, Science and Culture of Japan.

References

(1) Tokumaru S.: "Electrically Small Antenna", Trans. IEICE, **J71-B**, 11, pp. 1206-1212 (Nov. 1988).
(2) Newman E. H. and Pozar D. M.: "Electromagnetic Modeling of Composite Wire and Surface Geometries", IEEE Trans. Antenna & Propag., **AP-26**, 6, pp. 784-789 (Nov. 1978).
(3) Richmond J. H.: "Wire-Grid Model for Scattering by Conducting Bodies", IEEE Trans. Antennas & Propag., **AP-14**, 6, pp. 782-786 (Nov. 1966).
(4) Amano N., Doi T. and Sato R.: "Matrix Method for Analysis of A Curved-Wire-Antenna Using the Mutual Impedance between Two V-Shape Antennas", Trans. IECE Japan, **58-B**, 5, pp. 239-246 (May 1975).
(5) Richmond J. H. and Geary N. H.: "Mutual Impedance of Nonplanar-Skew Sinusoidal Dipoles", IEEE Trans. Antennas & Propag., **AP-23**, 3, pp. 412-414 (May 1975).
(6) Tilston M. A. and Balmain K. G.: "On the Suppression of Asymmetric Artifacts Arising in an Implementation of Thin-Wire Method", IEEE Trans. Antennas & Propag., **38**, 2, pp. 281-285 (Feb. 1990).
(7) Sato K., Matsumoto K., Fujimoto K., and Hirasawa K.: "Characteristics of a Planar Inverted-F Antenna on a Rectangular Conducing Body", Trans. IEICE, **J71-B**, 11, pp. 1237-1243 (Nov. 1988).
(8) Morishita H., Fujimoto K., and Hirasawa K.: "Analysis of Rectangular Microstrip Antenna Having the Same Width as the Ground Plane", Trans. IEICE, **J71-B**, 11, pp. 1274-1280 (Nov. 1988).
(9) Richmond J. H.: "Radiation and Scattering by Thin-Wire Structures in Complex Frequency Domain", Report 2902-10, The Ohio University Electro-Science Labo. (July 1973).
(10) Rumsey V. H.: "The Reaction Concept in Electromagnetic Theory", Phys. Rev., **94**, pp. 1483-1491 (June 1954); Also see errata, **95**, p. 1705 (Sept. 1954).
(11) Kraus J. D.: "Antennas" (2nd edition), p. 368, McGraw-Hill, New York (1988).
(12) Pozar D. M.: "Microwave Engineering", Addision-Wesley, New York (1990).

Nozomu Ishii was born in Sapporo, Japan, on October 8, 1966. He received the B. S. and M. S. degrees from Hokkaido University, Sapporo, Japan, in 1989 and 1991 respectively. In 1991, he joined the faculty of Engineering at Hokkaido University, where he is currently a Research Associate of Electronic Engineering. His current research interests are in the area of numerical analysis of small antenna. He is a member of the IEEE.

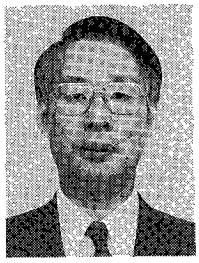

Kiyohiko Itoh was born in Sapporo, Japan, on May 15, 1939. He received the B. S. E. E., M. S., and Ph. D. degrees from Hokkaido University, Sapporo, Japan, in 1963, 1965, and 1973 respectively. Since 1965, he has been on the faculty of Engineering at Hokkaido University, where he is currently a Professor of Electronic Engineering. During 1970–1971, he was with the Department of Electrical and Computer Engineering, Syracuse University, Syracuse, NY, as a Research Associate, on leave from Hokkaido University. His special interests are in electromagnetic radiation, wave optics, mobile radio communications, and solar power satellites. He is a member of the IEEE and the Institute of Television Engineering of Japan.